Enhancement of Anti-Robo1 Immunotoxin Cytotoxicity to Head and Neck Squamous Cell Carcinoma via Photochemical Internalization

Noriko Komatsu[1,2,3], Kenichi Mitsui[2], Osamu Kusano-Arai[2,4], Hiroko Iwanari[2], Kazuto Hoshi[3], Tsuyoshi Takato[3,5], Takahiro Abe[3] and Takao Hamakubo[2*]

[1]Department of Sensory and Motor System Medicine, The University of Tokyo Graduate School of Medicine, Bunkyo-ku, Tokyo, Japan

[2]Department of Quantitative Biology and Medicine, Research Center for Advanced Science and Technology, The University of Tokyo, Meguro-ku, Tokyo, Japan

[3]Department of Oral and Maxillofacial Surgery, The University of Tokyo Hospital, 7-3-1 Hongo, Bunkyo-ku, Tokyo, Japan

[4]Institute of Immunology Co. Ltd., Bunkyo-ku, Tokyo, Japan

[5]JR Tokyo General Hospital, Shibuya-ku, Tokyo, Japan

***Corresponding author:** Takao Hamakubo, Department of Quantitative Biology and Medicine, Research Center for Advanced Science and Technology, The University of Tokyo, Meguro-ku, Tokyo, Japan, Tel: +81 3-5452-5231; E-mail: hamakubo@qbm.rcast.u-tokyo.ac.jp

Abstract

Background: Head and neck squamous cell carcinoma (HNSCC) is the sixth most common cancer worldwide. The long-term complications arising from standard therapy with surgery, chemotherapy and radiotherapy lower the quality of life (QOL) due to eating disorders, speech problems and cosmetic issues. Recently the importance of antibody therapy has increasingly come to be recognized for its capacity to enhance QOL. Robo1, an axon guidance receptor, has been received considerable attention as a monoclonal antibody target in various cancers.

Methods and findings: We checked the expression of Robo1 and the cytotoxic effect of saporin-conjugated anti-Robo1 immunotoxin (IT) against several HNSCC cell lines. The Robo1 cell surface expression level estimated by flow cytometry using the antibody B5209B was approximately 220,000 copies in Robo1 over-expressed CHO (Robo1/CHO) cells, and in HNSCCs, 22,000 copies in HSQ-89 cells, 3,000 copies in Sa3 cells, and few copies inSAS cells. Conventional IT treatment exhibited an inadequate cytotoxic effect even in HSQ-89 cells. When we added a photosensitizer and LED light illumination (650 nm), the cytotoxic effect was remarkably improved in HSQ89. With longer exposure, significant cytotoxicity was observed, even in Sa3 cells.

Conclusion: These results suggest that the photochemical internalization (PCI) is a promising method for augmenting the cytotoxicity of IT against tumors. The drug delivery system shown in this study should be applicable to other targets with low level expression on cancer cells, thus widening the therapeutic window in rare cancers.

Introduction

Head and neck squamous cell carcinoma (HNSCC) is the sixth most common cancer worldwide [1,2]. The morbidity and mortality rates have changed little over the last 30 years [3]. In addition to the death rate, a major problem is that conventional treatments such as surgery, radiotherapy, and chemotherapy result in long-term functional decline, such as eating disorders, speech problems, and cosmetic issues resulting in a diminished quality of life (QOL) [4]. Thus, the development of novel treatments to minimize these treatment-related complications is an urgent issue. Monoclonal antibody treatment is one of the expected means to fulfilling this issue, but the effect of monoclonal antibody is still insufficient for solid tumors.

Robo1 was initially discovered as an axon guidance receptor in *Drosophila* [5]. The Robo family consists of Robo1-4 [6]. Human Robo1 has five immunoglobulin-like domains and three fibronectin III-like domains in its extracellular portion [6]. The first report of Robo1 as a tumor-specific antigen was in liver cancer [7], but it is now known to be expressed in a wide range of cancers, such as colon, breast, pancreatic, and lung cancer, and the squamous cell carcinoma of the head and neck [8,9]. It has been reported that the Slit2/Robo1 signal in cancer plays important roles in invasion, migration, the epithelial-

mesenchymal transition [8], and tumor-induced angiogenesis [8,9]. Recently, the antibody drugs, Cetuximab and Nivolumab, have been approved for HNSCC treatment by the Food and Drug Administration (FDA) [10,11]. On the other hand, Trastuzumab-DM1 (Pertuzumab) was approved by the FDA in 1998 for use in metastatic breast cancer [12]. As the progress of new generation antibody drug conjugates (ADCs) widens the therapeutic window, the combination therapy with immune checkpoint manipulation is now in clinical trial [13].

Photochemical internalization (PCI) is a relatively new method which is based on photosensitizers and light illumination of a specific wavelength to react with them. Photosensitizer activation by light induces a photochemical reaction that generates singlet oxygen ($^1O_2$) resulting in the destruction of endocytic membranes [14]. This approach is much more highly selective than ADCs due to its capacity to respond to localized irradiation. The technology is currently in a Phase I/II clinical trial using disulfonated tetraphenyl chlorin ($TPCS_{2a}$) as a new generation photosensitizer. In this study we used disulfonated aluminum phthalocyanine ($AlPcS_{2a}$), which has previously been utilized for photochemical drug delivery [15]. Here we report Robo1-targeting IT of Robo1-saporin with PCI in HNSCC. The results suggest that Robo1 comprises a novel immunotherapeutic target in HNSCC by the application of PCI, and the drug delivery system developed here should prove to be applicable to other targets of low abundance in cancer cells, thus widening the therapeutic window in rare cancers.

Materials and Methods

Cell culture

The HNSCC cell lines, HSQ-89 (derived from the maxillary sinus, RCB0789), HO-1-u-1 (derived from the floor of the mouth, RCB2102), Sa3 (derived from the upper gingiva, RCB0980), and SAS (derived from the tongue, RCB1974) were purchased from RIKEN (Saitama, Japan). HSQ-89 cells were cultured in Dalbecco's Modified Eagles Medium (DMEM) supplemented with 10% fetal bovine serum (FBS). HO-1-u-1 and SAS cells were cultured in RPMI1640 supplemented with 10% FBS. Sa3 cells were cultured in Basic Minimum Essential Medium (BME) supplemented with 20% newborn bovine serum (NBS). A Chinese hamster ovary (CHO) cell line (CHO-K1, CCl-61) was obtained from the American Type Culture Collection (Bethesda, MD). Robo1 stably overexpressing-CHO (Robo1/CHO) and Robo4 stably overexpressing-CHO (Robo4/CHO) cell lines were established with a Flp-In gene expression System (Thermo Scientific, MA), as described previously [16]. Robo1/CHO and Robo4/CHO cells were cultured in Ham's F-12 medium supplemented with 10% FBS.

Reverse transcription real-time PCR

Total RNA was isolated from cultured cells using an RNeasy Plus Mini Kit (Qiagen, Germany). To evaluate the mRNA expression level, reverse transcription of the target mRNA followed by quantitative real-time PCR (qPCR) was performed using a SuperScript™ III First-Strand Synthesis System (Thermo Scientific, MA) and SYBR Green PCR master mix (Takara, Japan).

The expression level of the target RNA was presented as the relative ratio of the threshold cycle (Ct) value normalized with Glyceraldehyde-3-phosphate dehydrogenase (GAPDH) RNA.

Western blot analysis

The protein mixture from the cell lysate (7.5 µg per lane, except for 0.75 µg in the case of Robo1/CHO) was subjected to SDS-PAGE using 10% acrylamide gel and electrically transferred to a nitrocellulose membrane (GE Healthcare Life Science, UK). After blocking with Block Ace (DS Pharma, Osaka, Japan) for 1h, the membrane was incubated with the anti-Robo1 monoclonal antibody A7241A (1.0 µg/ml, generated in-house) as the primary antibody for 2 h [7]. A horseradish peroxidase conjugated-goat anti mouse IgG antibody (Jackson Lab, ME) diluted to 1: 5,000 was used as the secondary antibody. The Robo1 band on the membrane was visualized by chemiluminescence using Super-signal West Dura Extended Duration Substrate (Thermo Scientific, MA) and an ImageQuant LAS 500 apparatus (GE Healthcare Life Sciences, UK).

RNA interference

RNA interference was performed with Lipofectamine RNAiMAX Reagent (Thermo Scientific, MA) according to the manufacturer's instructions. Briefly, 5×10^3 cells/well in 6-well plates were treated with 200 nM of each siRNA along with the RNAiMAX Reagent. After 40h incubation, Robo1 expression was examined by Western blot analysis. The targeting site of the Robo1 mRNA was

5'-UAUCGAGUUUCAUUGCCCAGACACCGGUGUCUGGGCAAUGAAACUCGAUA-3'.

The negative control (here-after si-Control; Stealth RNAi Negative Control Kit) was purchased from Thermo Scientific (MA).

Flow cytometry

Cells were seeded at 1×10^6 cells per well in a 96-well plate. The plate was centrifuged at 2,000 rpm at 4°C for 2 min, and then supernatants were removed. The cells were suspended and incubated with 1 µg of the monoclonal anti-Robo1 antibody (B5209B, generated in-house) [16,17] or Hyb3423 as a negative control in 100 µl sorting buffer (PBS containing 1% bovine serum albumin (BSA), 0.1 mM ethylenediaminetetraacetic acid (EDTA), and 0.1% Proclin300) for 60 min on ice, then washed with sorting buffer. Cells were subsequently incubated with R-Phycoerythin AffiniPure F(ab')2 Fragment Goat Anti Mouse IgG antibody (Jackson Lab, ME) for 60 min on ice. The cells were washed and resuspended in sorting buffer, then analyzed with Guava EasyCyte plus Flow cytometer (Merck, GKeA, Germany).

The expression level of Robo1 (copies/cell) was calculated from a histogram of a QIFKIT (Agilent Technologies, CA), as previously described [18].
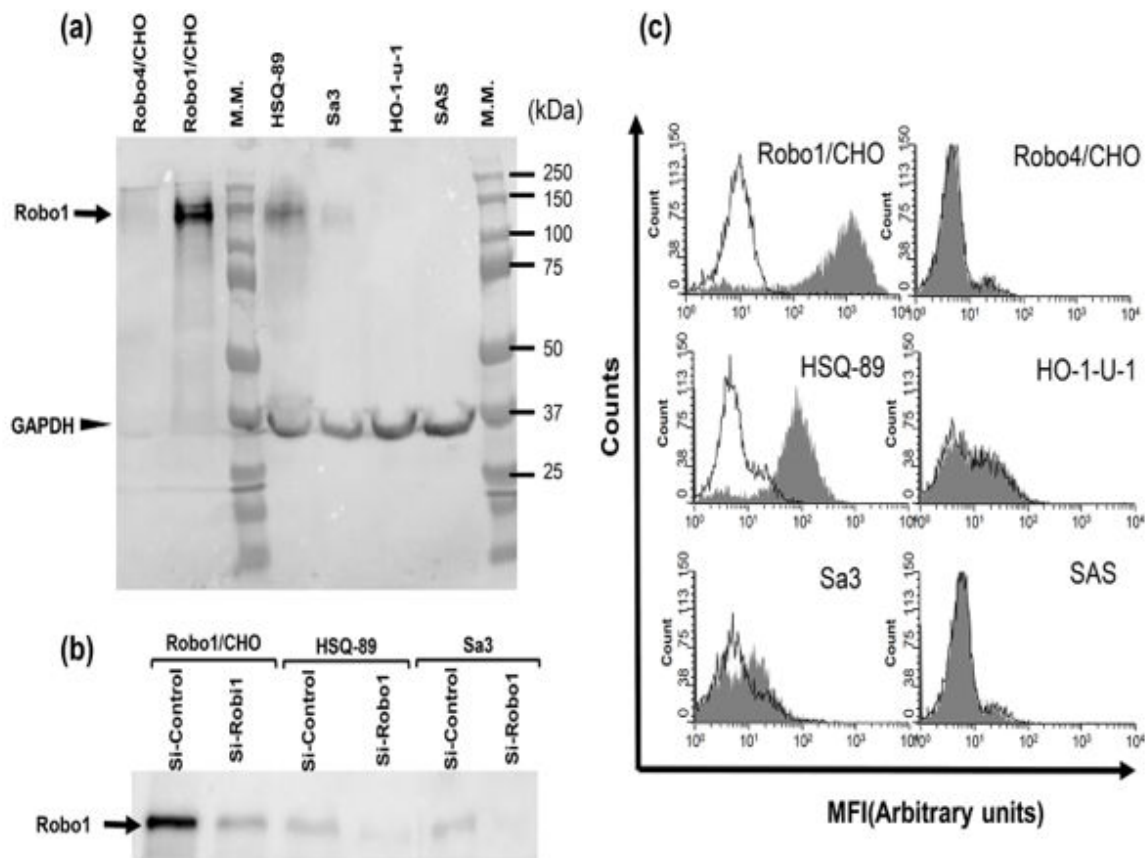

Figure 1 (a, b) The Robo1 protein band was detected in HSQ-89 and Sa3, both were decreased by specific siRNA treatment. **(c)** The Robo1 expression level on the cell surface estimated by flow cytometric analysis.

Table 1 The expression levels of the Robo1 protein correlated well with the mRNA expression level in each of the cell lines.

Cell lines	Robo1 mRNA (relative ratio to GAPDH)	Robo1 protein (molecules/cell)
Robo1/CHO	1.97 ± 0.798	220,000 ±15,800
HSQ-89	0.281 ± 0.389	22,300 ± 4,900
Sa3	0.0226 ± 0.00687	3,010 ± 138
HO-1-u-1	ND	184 ± 80.6
SAS	ND	33.7 ± 67.0
Robo4/CHO	ND	ND

Values are designated as means ± SD from three independent experiments.

ND: Non-Detected.

Immunotoxin cytotoxicity assay

A Saporin-conjugated anti-Robo1 antibody (B5209B) and Saporin-conjugated negative control antibody (B8109B), hereafter called IT-Robo1 and IT-NC, respectively, were prepared by incubating 2 µl of 1.1 µM streptavidin-saporin (Biotin-Z Internalization Kit [KIT-27-Z], Advanced Targeting Systems, CA) and 2 µl of 1.1 µM biotinylated monoclonal antibodies for 30 min at room temperature. Robo1/CHO and HSQ-89 cells were seeded at 2.5×10^3 cells per well in 96-well plates and cultured overnight, and then were exposed to various concentrations (0.0013 - 4.2 nM) of IT-Robo1 or IT-NC for either 72 h shown in **Figure 2a** or 168 h **Figure 2b**, respectively.

Cell viability was evaluated by adding 10 µl/well of CCK-8 solution (Cell Counting Kit-8, Dojindo Laboratory, Japan) and measuring the absorbance at 450 nm of each sample after 40 min to 2 h incubation, according to the manufacturer's instructions.

Cell viability was calculated using the following formula:

Cell viability (%) = $(a-c)/(b-c) \times 100$

where a represents the absorbance value of each sample, b the absorbance value for the IT free sample, and c the absorbance value of the blank sample (medium only) [19]. The means ± SD of the cell viability values were calculated from 3 independent experiments and plotted on the graph versus the

IT concentration. The IC_{50} values, i.e., the concentrations inhibiting protein synthesis by 50%, were evaluated from sigmoidal curves fitted to the plotted means using the generalized reduced gradient non-linear solving method in Excel software.
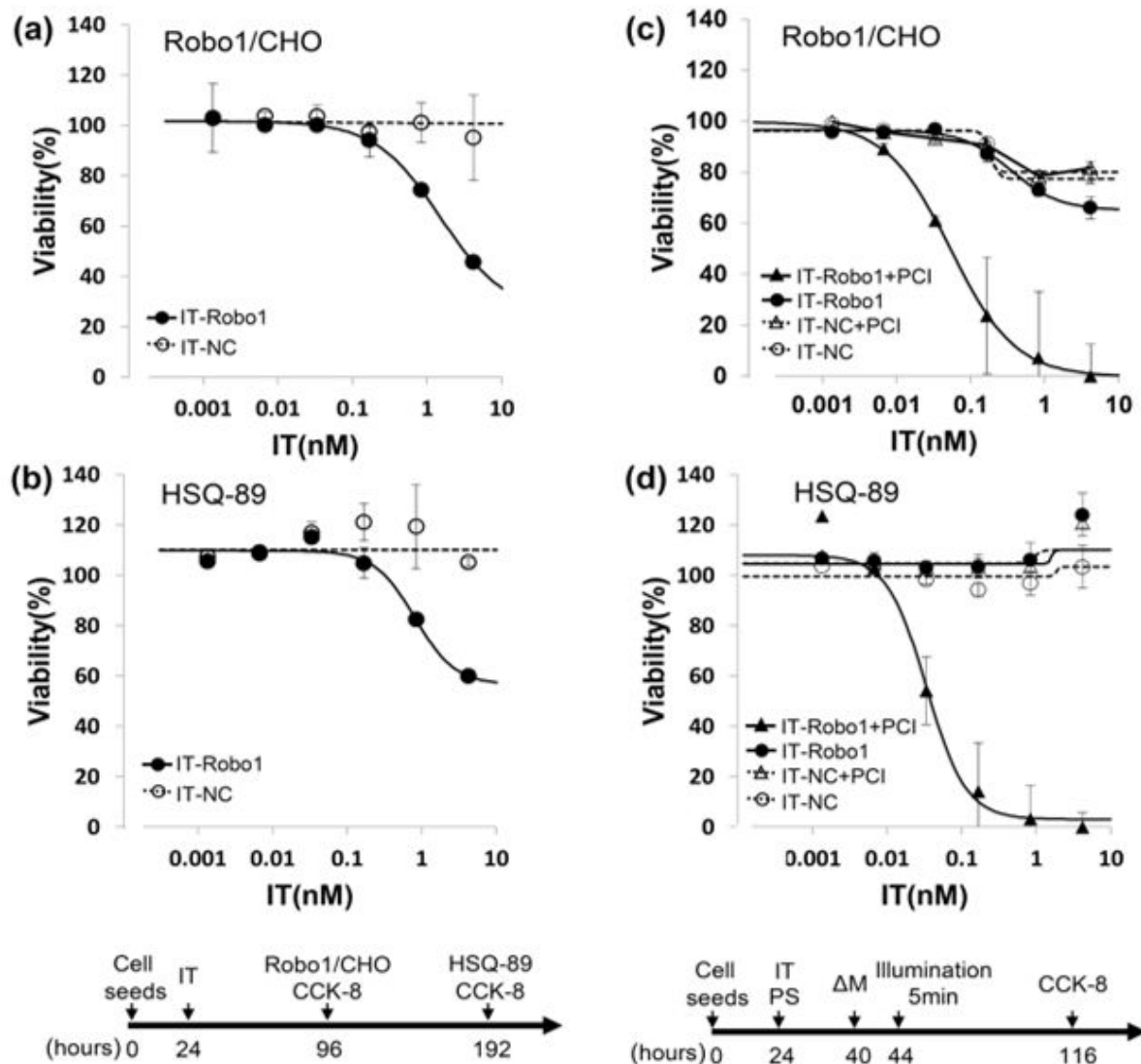

Figure 2 (a) The cytotoxic activity of IT-Robo1 to Robo1/CHO was Robo1-specific and dose-dependent. **(b)** The cytotoxicity of IT-Robo1. **(c)** The cytotoxic effect and the IC_{50} of IT-Robo1. **(d)** The dose-dependency of the PCI effect was much more conspicuous in HSQ-89 cells, where the IC_{50} was approximately 34 pM.

Cytotoxicity assay by PCI

The photosensitizer, disulfonated aluminum phthalocyanine, having sulfonate groups on adjacent phthalate rings ($AlPcS_{2a}$), was purchased from Frontier Scientific. A light-emitting diode (LED) lamp (54 W) with a peak wavelength 650 nm was purchased from King Do Way (18PCS E27, Amazon.co.jp).

Cells were seeded at 2.5×10^3 cells (Robo1/CHO), 5.0×10^3 cells (SAS) or 2.0×10^4 cells (HSQ-89, Sa3) per well in 96-well plates and cultured at 37°C overnight. The optimum concentration of $AlPcS_{2a}$ was examined for each cell line independently. Based on the results, $AlPcS_{2a}$ at a final concentration of 5.0 μg/ml was used in Robo1/CHO, HSQ-89 and Sa3, while 0.5 μg/ml was used in SAS for the cytotoxicity experiments. Along with the photosensitizer, the immunotoxin, IT-Robo1 or IT-NC, was added to each well at a final concentration between 0.0013-4.2 nM and incubated for 16 h. Then the culture medium was changed to the drug free medium. After 4 h culture, the cells were exposed to illumination from an LED lamp for 5 min (62.7 mW/cm², 18.8 J/cm²). After 72 h, cell viability was assessed with a CCK-8 kit, as described in the section on the IT cytotoxicity assay. A longer exposure, 10min, was applied for Sa3 and SAS (62.7 mW/cm², 37.6 J/cm²). IC_{50} values were calculated as described in the IT cytotoxicity assay.

Statistical analysis

Data are shown as the means ± SD. Statistical evaluation was performed using analysis of variance (ANOVA) followed by Tukey Honest Significant Differences test. p-value of <0.01 was taken to be statistically significant.

Results

The expression of Robo1 in various HNSCC cells

The expression level of Robo1 mRNA were examined by qPCR, as described in materials and methods. The protein level of Robo1 on the surface of each cell was estimated by Western blot and flow cytometry with the specific antibodies A7241A and B5209B, respectively. The Robo1 protein band was detected in HSQ-89 and Sa3 cells at approximately 200 kDa, both were decreased by specific siRNA **(Figures 1a and 1b)** treatment. The expression levels of the Robo1 proteins correlated well with the mRNA level in each of the cell lines **(Table 1)**. The Robo1 expression level on the cell surface estimated by flow cytometric analysis **(Figure 1c)** was approximately 220,000 copies in Robo1/CHO, 22,000 copies in HSQ89, 3,000 copies in Sa3, and 200 copies in HO-1-u-1, respectively, but there were few copies in SAS cells **(Table 1)**. These expression levels of the Robo1 protein correlated well with the mRNA expression level in each of the cell lines, as shown in **Table 1.**
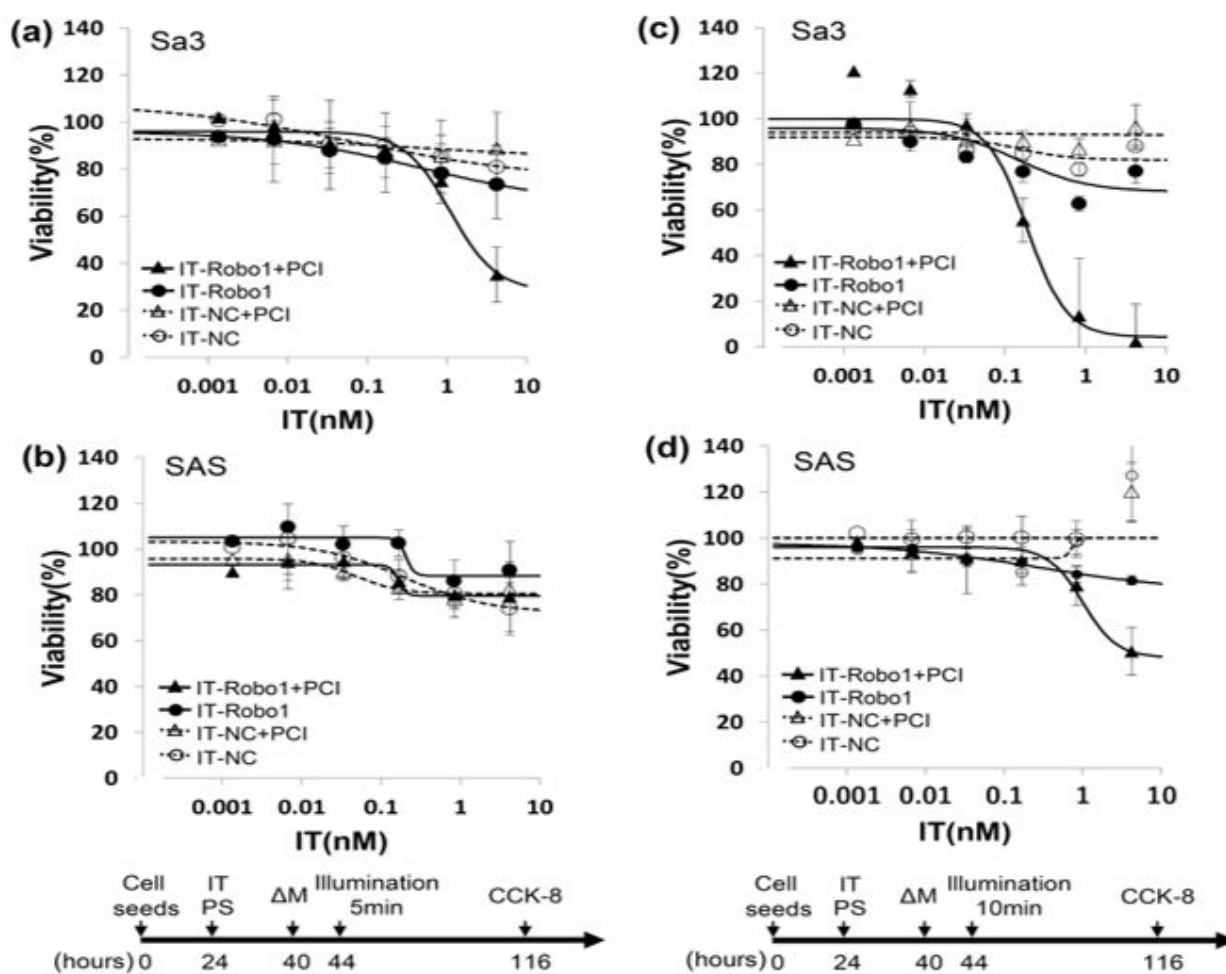

Figure 3 (a, b) The IT-Robo1. **(c)** the cytotoxic effect of Sa3 **(d)** In SAS, a significant cytotoxic effect was not observed.

Increase in the anti-Robo1 antibody immunotoxin (IT-Robo1) cytotoxic activity by photochemical internalization (PCI)

The cytotoxic activity of IT-Robo1 to Robo1/CHO was Robo1-specific and dose-dependent **(Figure 2a)**. However, the effect at most was 60%, even at the highest IT concentration (4.2 nM) **(Figure 2a)**. This result suggested an insufficient internalization of IT-Robo1. The cytotoxicity of IT-Robo1 was less effective in HSQ-89 cells, of which the cytotoxicity reached a maximum of 40% at the highest concentration **(Figure 2b)**.

To increase the internalization of IT-Robo1, we utilized AlPcS$_{2a}$, which has been used to disrupt endosomes via the formation of reactive oxygen species by light irradiation. First, we examined the cytotoxicity of AlPcS$_{2a}$ itself to determine the appropriate concentration for each cell line. All cell lines

except SAS displayed a similar dose-dependent vulnerability to $AlPcS_{2a}$. SAS is much more susceptible to photosensitizer treatment, so we performed the PCI experiment using 0.5 µg/ml for SAS and 5.0 µg/ml for the other cells.

The addition of $AlPcS_{2a}$ to the medium for 16 h followed by 670 nm LED illumination for 5 min resulted in sufficient cytotoxicity in the presence of IT-Robo1 in Robo1/CHO. The cytotoxic effect was dose-dependent (ANOVA) and the IC_{50} of IT-Robo1 was approximately 54 pM **(Figure 2c)**. The dose-dependency of the PCI effect was much more conspicuous in HSQ-89 cells, where the IC_{50} was approximately 34 pM **(Figure 2d)**.

The low Robo1 expression cell line Sa3 becomes susceptible to IT and PCI with longer exposure

As the Robo1 expression levels in Sa3 and SAS were low, about at 3,000 copies and 30 copies, respectively, by flow-cytometry evaluation **(Table 1),** the IT-Robo1 effects were not seen at 5 min exposure **(Figures 3a and 3b)**. However, when the exposure to light was prolonged to 10 min, which doubled the energy, a significant, dose-dependent cytotoxic effect was clearly evident in Sa3 **(Figure 3c)** (ANOVA with post-hoc Tukey HSD test, p=0.00061). In SAS, a significant cytotoxic effect was not observed, even with longer exposure **(Figure 3d)** (ANOVA, p=0.0196).

Discussion

Maiti et al. demonstrated a moderate to high expression level of Robo1 protein in contrast to a decreased expression level of Robo1 mRNA in head and neck carcinoma [20]. Zhao et al. demonstrated that Slit2/Robo1 signaling promoted the adhesion, invasion and migration of tongue carcinoma cells via downregulation of E-cadherin [8]. A similar effect of Slit/Robo1 signaling blockade in colorectal epithelial cell carcinogenesis was suggested by Zhou et al. [21]. Thus, Robo1 is a good target for antibody therapy in cases of highly expressed protein.

In our study, the expression levels of Robo1 mRNA and protein were well correlated in the squamous carcinoma cells tested. The discrepancy with the mRNA level reported by Maiti et al. may be due to the samples used [20]. The cell lines we used, such as HepG2 [7], HUVECs [22], and SCCs of the lung [23], displayed well correlated levels of mRNA and protein expression.

As the newer generation of ADCs has been greatly improved in their effect on solid tumors [13], we checked the availability of toxin-conjugated anti-Robo1monoclonal antibodies to oral carcinoma cells. The immunotoxin IT-Robo1 prepared by conjugating saporin to the high affinity antibody B5209B against Robo1 (Kd =30 pM) [16,17] displayed an inadequate cytotoxic activity, even against the over-expressed Robo1/CHO cells **(Figures 2a and 2b)**. This result suggested the possibility that the internalization of IT-Robo1 was insufficient. Thus, we undertook further testing of the photosensitizer, AlPcS2a, which reportedly enhances endosomal disruption through the

generation of singlet oxygen by irradiation with light. We found 5 min exposure of red light (650 nm LED, 62.7 mW/cm^2, 18.8 J/cm^2) to be sufficient for the effective killing of approximately 20,000 copies/cell in Robo1 expressed HSQ-89 cells (IC_{50} = 0.034 nM) **(Figure 2)**. Considering the fact that the IC_{50} values of EGFR- and EGFRvIII-specific bivalent recombinant IT (DT390-BiscFv806) against various HNSCC cell lines are reported to be 0.24 nM ~156 nM [24], the results here suggest IT-Robo1 with $AlPcS_{2a}$ has sufficient efficacy for clinical applications.

It is remarkable that the effective cytotoxicity in Sa3 cells was achieved just by doubling the exposure time to 10 min. Since the expression level of surface Robo 1 is estimated to be only 3,000 copies/cell in this cell line, these results suggest IT-PCI therapy may prove effective in a broad range of HNSCCs, possibly including even dysplasia, which is reported to have a low to moderate expression of the Robo1 protein [20].

Conclusion

The use of PCI in combination with the cancer drug bleomycin reportedly induced a synergistic inhibition of tumor growth in two different tumor models [25]. Bostad et al. has reported that the cancer stem cell marker CD133-targeting immunotoxin AC133-saporin exhibited efficient cytotoxic activity and tumor growth inhibition only when treated with PCI [26]. Thus, the technique demonstrates the possibility of a site-specific and minimally invasive therapeutic strategy for cancer.

In this study it is demonstrated that PCI combined with IT confers a robust cytotoxic activity on IT which previously was inadequate because of problems with internalization. Moreover, the cytotoxic effects were enhanced by longer exposure to illumination, suggesting the utility of this technique for other targets of low abundance on cancer cells. Thus, it is expected to widen the therapeutic window in rear cancers.

Acknowledgements

References

1. Jacques F, Hai-Rim S, Freddie B, David F, Colin M, et al. (2010) Estimates of worldwide burden of cancer in 2008: GLOBOCAN 2008. Int J Cancer 127: 2893-2917.

2. Jemal A, Bray F, Center MM, Ferlay J, Ward E, et al. (2011) Global Cancer Statistics. Ca Cancer J Clin 61: 69-90.

3. Chan LP, Wang LF, Chiang FY, Lee KW, Kuo PL, et al. (2016) IL-8 promotes HNSCC progression on CXCR1/2-meidated NOD1/RIP2 signaling pathway. Oncotarget 7: 61820-61831.

4. Thomson PJ, Wylie J (2002) Interventional laser surgery: An effective surgical and diagnostic tool in oral precancer management. Int J Oral Maxillofac Surg 31: 145-153.

5. Kidd T, Brose K, Mitchell KJ, Fetter RD, Tessier-Lavigne M, et al. (1998) Roundabout controls axon crossing of the CNS midline and defines a novel subfamily of evolutionarily conserved guidance receptors, Cell 92: 205-215.

6. Ballard MS, Hinck L (2012) A roundabout way to cancer, In: Academic Press, Ira O. Daar (Ed.), Adv Cancer Res 114: 187-235.

7. Ito H, Funahashi S, Yamauchi N, Shibahara J, Midorikawa Y, et al. (2006) Identification of ROBO1 as a novel hepatocellular carcinoma antigen and a potential therapeutic and diagnostic target. Clin Cancer Res 12: 3257-3264.

8. Zhao Y, Zhou FL, Li WP, Wang J, WANG LJ (2016) Slit2-Robo1 signaling promotes the adhesion, invasion and migration of tongue carcinoma cells via upregulating matrix metalloproteinases 2 and 9, and downregulating E-cadherin. Molecular Medicine Reports 14: 1901-1906.

9. Wang B, Xiao Y, Ding BB, Zhang N, Yuan Xb, et al. (2003) Induction of tumor angiogenesis by Slit-Robo signaling and inhibition of cancer growth by blocking Robo activity. Cancer Cell 4: 19-29.

10. Blasco MA, Svider PF, Raza SN, Jacobs JR, Folbe AJ, et al. (2017) Systemic therapy for head and neck squamous cell carcinoma: Historical perspectives and recent breakthroughs. Laryngoscope pp. 1-5.

11. Zagouri F, Terpos E, Kastritis E, Dimopoulos MA (2016) Emerging antibodies for the treatment of multiple myeloma, Expert Opin. Emerg. Drugs 21: 225-37.

12. Smith I, Procter M, Gelber RD, Guillaume S, Feyereislova A, et al. (2007) 2-year follow-up of trastuzumab after adjuvant chemotherapy in HER2-positive breast cancer: A randomised controlled trial. Lancet 369: 29-36.

13. Thomas A, Teicher BA, Hassan R (2016) Antibody-drug conjugates for cancer therapy. Lancet Oncol 17: 254-262.

14. Berg K, Weyergang A, Prasmickaite L, Bonsted A, Hogset A, et al. (2010) Photochemical Internalization (PCI): A Technology for Drug Delivery. Photodynamic Therapy MIMB 635: 133-145.

15. Berg K, Nordstrand S, Selbo PK, Tran DT, Angell-Petersen E, et al. (2011) Disulfonated tetraphenyl chlorin (TPCS2a), a novel photosensitizer developed for clinical utilization of photochemical internalization. Photochem. Photobiol. Sci 10: 1637-51.

16. Fujiwara K, Koyama K, Suga K, Ikemura M, Saito Y, et al. (2014) A 90Y-labelled anti-ROBO1 monoclonal antibody exhibits antitumour activity against hepatocellular carcinoma xenografts during ROBO1-targeted radioimmunotherapy. EJNMMI Res 4.

17. Kusano-Arai O, Fukuda R, Kamiya W, Iwanari H, Hamakubo T (2016) Kinetic exclusion assay of monoclonal antibody affinity to the membrane protein Roundabout 1 displayed on baculovirus, Anal Biochem 1: 41-49.

18. Kusano-Arai O, Iwanari H, Mochizuki Y, Nakata H, Kodama T, et al. (2012) Evaluation of the asparagine synthetase level in leukemia cells by monoclonal antibodies. Hybridoma (Larchmt) 31: 325-32.

19. Shimizu M, Imai M (2008) Effect of the antibody immunotherapy by the anti-MUC1 monoclonal antibody to the oral squamous cell carcinoma in vitro. Biol Pharm Bull 31: 2288-93.

20. Maiti GP, Ghosh A, Mondal P, Ghosh S, Chakraborty J, et al. (2015) Frequent inactivation of SLIT2 and ROBO1 signaling in head and neck lesions: clinical and prognostic implications. JOMFP 119: 202-212.

21. Zhou WJ, Geng ZH, Chi S, Zhang W, Niu XF, et al. (2011) Slit-Robo signaling induces malignant transformation through Hakai-mediated E-cadherin degradation during colorectal epithelial cell carcinogenesis, Cell Res 21: 609-626.

22. Enomoto S, Mitsui K, Kawamura T, Iwanari H, Daigo K, et al. (2015) Suppression of Slit2/Robo1 mediated HUVEC migration by Robo4, Biochem Biophys Res Commun 469: 707-802.

23. Fujiwara K, Koyama K, Suga K, Ikemura M, Saito Y, et al. (2015) 90Y-labeled anti-ROBO1 monoclonal antibody exhibits antitumor activity against small cell lung cancer xenografts. PLoS One 10: 1-13.

24. Meng J, Liu Y, Gao S, Lin S, Gu X, et al. (2015) A bivalent recombinant immunotoxin with high potency against tumors with EGFR and EGFRvIII expression, Cancer Biol Ther 16: 1764-1774.

25. Berg K, Dietze A, Kaalhus O, Hogset A (2005) Site-specific drug delivery by photochemical internalization enhances the antitumor effect of bleomycin. Clin Cancer Res 11: 8477-8485.

26. Bostad M, Olsen CE, Peng Q, Berg K, Hogset A, et al. (2015) Light-controlled endosomal escape of the novel CD133-targeting immunotoxin AC133-saporin by photochemical internalization - A minimally invasive cancer stem cell-targeting strategy. J Control Release 28: 37-48.